ChemComm

Accepted Manuscript

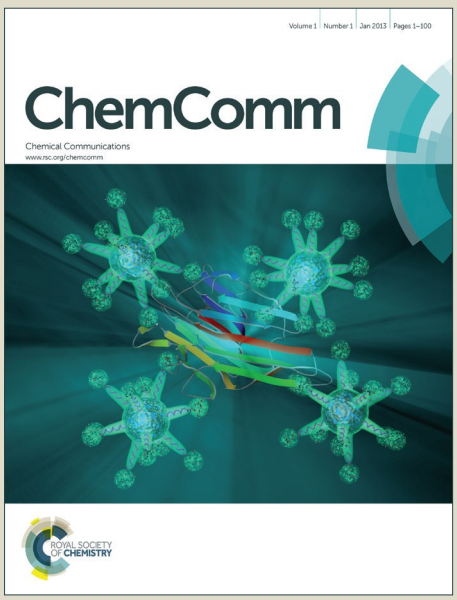

ROYAL SOCIETY OF CHEMISTRY

www.rsc.org/chemcomm

Journal Name

COMMUNICATION

Evidence of Single-Nanoparticle Translocation through Solid-State Nanopore by Plasmon Resonance Energy Transfer

Received 00th January 20xx,
Accepted 00th January 20xx

DOI: 10.1039/x0xx00000x

www.rsc.org/

Yue Cao[a], Yao Lin[a], Ruo-Can Qian[a]*, Yi-Lun Ying[a]*, Wei Si[b], Jingjie Sha[b]*, Yunfei Chen[b], Yi-Tao Long[a]*

This work proposes a gold nanoparticle (AuNP) based probe to study the single-nanoparticle translocation behavior through a silicon nitride (SiNx) solid-state nanopore. The AuNP probe is functionalized with a rhodamine derivative molecule, termed Rhod-DPA, whose fluorescence can be activated at the presence of Cu^{2+} due to the binding between Rhod-DPA and Cu^{2+}. The Cu^{2+} triggered configuration change of Rhod-DPA on probe surface can induce the plasmon resonance energy transfer (PRET) from single AuNPs to the transformed fluorescent molecules, which can be detected by the color change of AuNP probes under dark-field microscopy (DFM) and their scattering spectra recorded by a spectrometer. By analyzing the peak shifts before and after the addition of Cu^{2+}, the evidence of single nanoparticle translocation through the nanopore has been obtained, proving the successful establishment of the tracking strategy.

Solid-state nanopores, generally prepared with silicon nitride (SiNx), has been widely applied in single molecule analysis.[1-7] Previous studies have reported the use of solid-state nanopores in the detection of single-strand deoxyribonucleic acid (DNA), proteins, peptides, host-guest molecules and etc.[8-12] Noticeably, nanopores have been found to owe the ability to trap nanoparticles, which has been used for the study of nanoparticle translocation.[13,14] Up to now, a variety of methods has been proposed for the characterization of the translocation behaviour, mainly including electrochemical analysis[15-18] and optical methods[19-21]. Generally, a typical experiment involves a nanopore placed between two chambers filling with solution containing an certain electrolyte.[22] Nanoparticles are dispensed in one chamber and a electrical field is added through the solution as the nanoparicles pass from one chamber to the other side through the nanopore, which can trigger a change in the current or the optical properties of the solution according to the different design.[23-26] However, these strategies fail to provide direct evidence to demonstrate the translocation of nanoparticles, thus it is still a challenge to develop strategies which can detect the particle translocation directly.

In this work, we present a method base on a special functionalized gold nanoparticle (AuNP) to discover the direct evidence of single AuNP translocation though a solid-state nanopore. A rhodamine derivative molecule, N-(3',6'-bis(diethylamino)-3-oxospiro[isoindoline-1,9'-xanthen]-2-yl)-5-(1,2-dithiolan-3-yl)pentanamide (Rhod-DPA) was designed and synthesized for the modification of AuNPs. Initially, Rhod-DPA was non-fluorescent. In the presence of Cu^{2+}, the fluorescence could be turned "on" due to the high affinity between the Rhod-DPA molecule and Cu^{2+} through the amide bond. As shown in Figure 1, the 50 nm AuNPs were functionalized with Rhod-DPA through its dithiol group (S-S) to obtain the AuNP probe.

Here, a nanopore cell, which was composed by two chambers connected with a SiNx solid-state nanopore (~100 nm), was used to perform the AuNP translocation experiments. After both of the chambers were filled with 10 mM KCl, AuNP probes were added into the *cis* side and a potential was added to the electrode at the left chamber. Under the effect of the electrical field, the AuNP probes translocated from the *cis* side to the *trans* side. After that, Cu^{2+} was added to the *trans* chamber. Once the probe passed through the nanopore and met Cu^{2+}, the configuration of Rhod-DPA molecule on AuNP surface was changed due to the specific conjugation between Cu^{2+} and Rhod-DPA, thus turned on the fluorescence of Rhod-DPA molecules and triggered a plasmon resonance energy transfer (PRET)[27-29] from AuNP cores to Rhod-DPA. The PRET effect could be observed by color changes of AuNP probes under dark-field microscopy (DFM) and the peak intensity of scattering spectra, which could be considered as the firm evidence of the translocation of AuNP probes. With the proposed method, the PRET variation before and after the translocation of nanoparticles has been successfully detected and analyzed.

[a] *Key Laboratory for Advanced Materials & Department of Chemistry, East China University of Science and Technology, Shanghai, 200237,*
[b] *Jiangsu Key Laboratory for Design and Fabrication of Micro-Nano Biomedical Instruments, School of Mechanical Engineering, Southeast University, Nanjing 211189, P. R.China.*
** Correspondence Authors: ytlong@ecust.edu.cn; ruocanqianecust@163.com; yilunying@ecust.edu.cn; major212@seu.edu.cn*
†Electronic Supplementary Information (ESI) available: Detailed description of the material, density functional theory calculations and supplementary experimental. See DOI: 10.1039/x0xx00000x

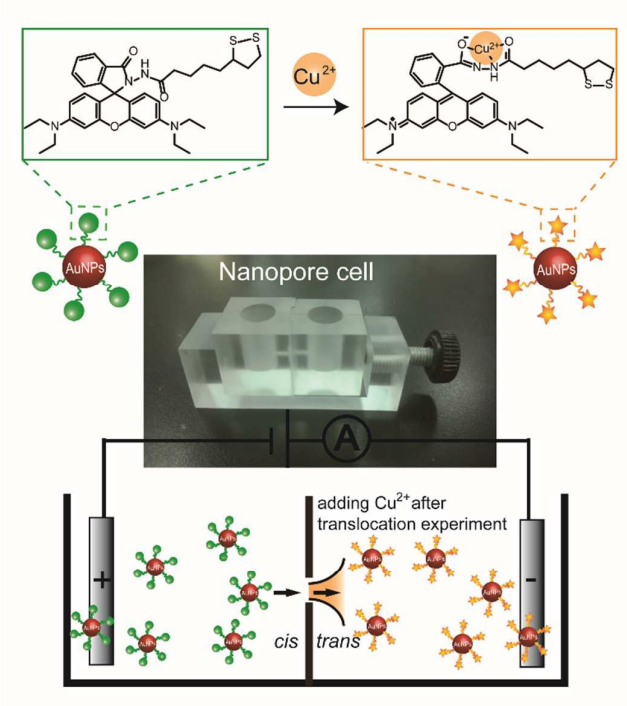

Figure 1. Schematic representation of the plasmon resonance energy transfer based on the single-nanoparticle translocation through solid-state nanopore

I-V response curve was first recorded for the characterization of the solid-state nanopore. As shown in Figure 2c, after the electrolyte solution (10 mM KCl) was added to *cis* and *trans* chambers, a linear relationship between the ionic current and applied voltage in the range of -0.9 V to 0.9 V was observed (R^2 = 0.99) with the corresponding pore conductance G calculated to be 4.79 nS.[22] The TEM image showed the diameter of the nanopore is 100 nm. To discuss the translocation events of the AuNP probes, we observe the time trace of the ionic current traces before and after the addition of AuNP probes (Figure 2a). Initially, in the absence of AuNP probes, no translocation events were observed. When AuNP probes were added to the *cis* chamber and applied a negative voltage, the translocation appeared as spikes in the current traces. At -500 mV, a few spikes emerged, indicating the AuNP probes translocate through the presented solid-state nanopore at a low frequency. While at -800 mV, intensive spikes with a higher current blockage were observed which confirmed the frequently translocation of AuNP probes at a more negative potential. The corresponding signals in a higher resolution are depicted in Figure 2b. The scatter plots of ΔI (peak current subtracted by background signal) vs. time duration of the blockage events were shown in Figure 2d at -500 mV and -800 mV respectively.

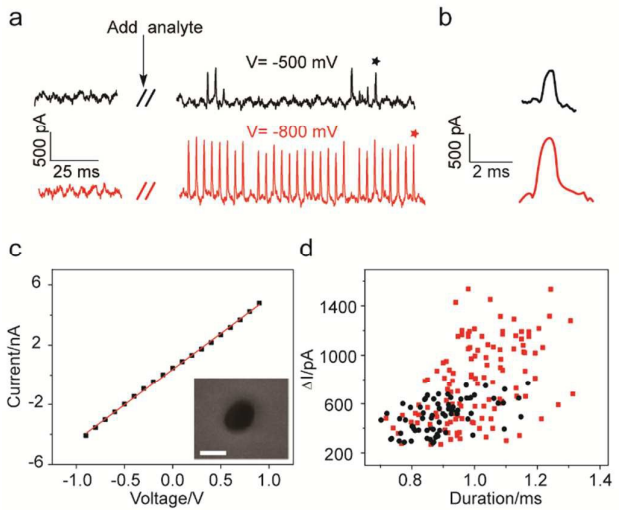

Figure 2. (a) Time trace of the ionic current through the nanopore before and after AuNP probes were added in the cis side at -500 mV (black) and -800 mV (red). (b) The detail of the current signals. (c) I-V curve of the nanopore. Inset: TEM image of the nanopore (scale bar: 100 nm). (d) Scatter plot of the blockage current vs. blockage duration at -500 mV (black) and -800 mV (red), respectively

Before the Cu^{2+} conjugation experiments, the Rhod-DPA and the AuNP probes were characterized. Rhod-DPA was synthesized[30] and characterized (Figure S1-3). Transmission electron microscopy (TEM) image showed a good distribution of Rhod-DPA modified AuNP probes with the diameter around 50 nm (Figure S4). The AuNP probes presented a positive Zeta potential (Figure S5), which was benefit for the translocation because the nanopore is negatively charged. Therefore, after a potential of -800 mV was added to the left electrode, the AuNP probes passed through the nanopore under the effect of external electric field. Afterwards, $CuSO_4$ solution (10 μL, 1 mM) was added to the right side. In the presence of Cu^{2+}, the Rhod-DPA-Cu^{2+} complex could be formed though the amide bond.[31] To demonstrate translocation of the AuNP probes, an indium tin oxide (ITO) slide was inserted into the right side during the electric field was existed. Then the slide was washed and sent for scanning electron microscope (SEM) detection. As shown in Figure 3a, scattered AuNP probes could be observed attaching on the ITO slide, confirming the translocation. Further analysis of the ITO slide by time-of-flight secondary ion mass spectrometry (ToF-SIMS) showed the existence of Cu^{2+} (Figure S6), indicating the linkage between Rhod-DPA and Cu^{2+}. In order to further study the conjugation of Cu^{2+}, the UV-Vis spectra of Rhod-DPA solution (500 μL, 0.1 mM) incubated with $CuSO_4$ solution (50 μL, 1 mM) for different times was observed. As shown in Figure 3b, the color of the solution gradually turned from colorless transparent to pink, and the absorption peak at 560 nm kept increasing with the incubation time. In addition, the fluorescence of the mixed solution emerged after 10 min (Figure S7), confirming the formation of the Rhod-DPA-Cu^{2+} complex.[32] Afterwards, DFM imaging (Figure 3c) and the scattering spectra (Figure 3d) were performed to test the PRET effect between AuNPs and Rhod-DPA-Cu^{2+} complex. It could be observed that the brightness intensity of the AuNP spots sharply decreased almost by half without noticeable spectral shift. These results indicated the translocation of AuNP probes and the following Cu^{2+} conjugation caused PRET effect, thus confirmed the successful

construction of the proposed system for obtaining the direct evidence of the nanoparticle transportation.

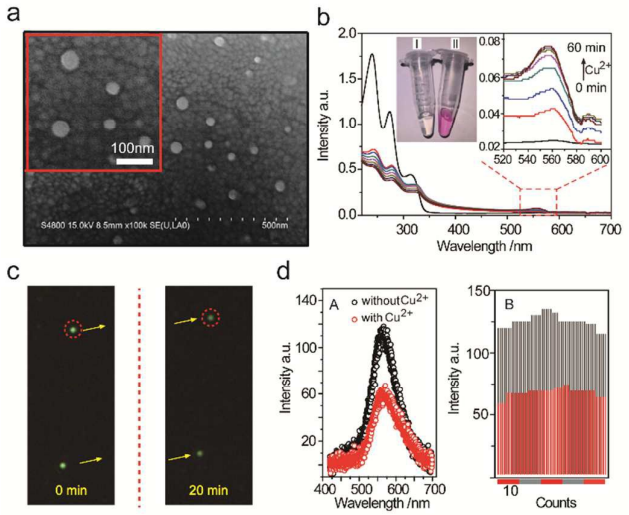

Figure 3. (a) The SEM image of Cu^{2+} conjugated AuNP probes captured on ITO slide (detail shown in the box on the top left corner). (b) UV-Vis spectra of Rhod-DPA after different incubation times with Cu^{2+} (detail shown in the box on the top right corner). Inset: photograph of Rhod-DPA before (transparent colour) and after (pink colour) the conjugation of Cu^{2+}. (c) DFM images of AuNP probes before (left) and after (right) the treatment of 1 mM Cu^{2+}. (d) (A) Corresponding scattering spectra of the AuNP probe in circle. (B) The statistical distribution of the scattering peak intensity before (black) and after (red) Cu^{2+} treatment.

To further discuss the selectivity of the Rhod-DPA modified AuNP probes for Cu^{2+}, a series of different interfering ions (Zn^{2+}, Pb^{2+}, Na^{+}, K^{+}, Hg^{2+}, Mg^{2+}, Ni^{2+}, Cd^{2+}, Ca^{2+}) and Cu^{2+} were used to perform the above translocation test. Briefly, after a negative potential (-800 mV) was added to the left side, a certain ion solution was added to the right side and an ITO slide was inserted. After 1 h, the ITO slide was taken out, rinsed with pure water and dried for DFM observation. The peak intensity on scattering spectra of AuNP probes before (I_{s0}) and after (I_{s1}) translocation were tested for the calculation of scattering spectra intensity changes ($\Delta I_s = I_{s1} - I_{s0}$). $\Delta I_s/I_{s0}$ value of each ion was calculated to evaluate the quenching effect, depending on the conjugation extent between the ion and Rhod-DPA. As shown in Figure 4a, no obvious scattering quenching was observed after the addition of interfering ions; while in the presence of Cu^{2+}, a significant change of the scattering intensity could be observed, demonstrating the favourable selectivity of Rhod-DPA for Cu^{2+}. Furthermore, a linear relationship was found between $\Delta I_s/I_{s0}$ value and the logarithm of Cu^{2+} concentration (Figure 4b). The scattering intensity of the single Rhod-DPA-modified AuNP decreased with the increasing Cu^{2+} concentration, about 30% at 1 nM Cu^{2+}, thus producing a low detection limit at ultratrace level (10^{-9} M) with high sensitivity. Kinetic studies showed that Cu^{2+} conjugated quickly with Rhod-DPA modified AuNPs with 10 min (Figure S8). In addition, a control experiment was performed using bare AuNPs (Figure S9), which showed no observable changes on scattering spectra before and after the addition of Cu^{2+}. The above results confirmed the specific recognition between Rhod-DPA and Cu^{2+}, and the PERT effect after the conjugation.

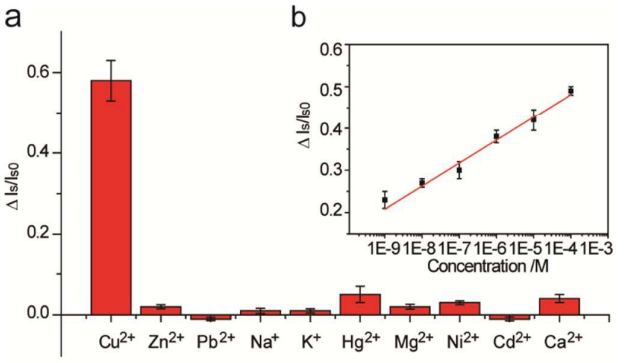

Figure 4. (a) Selectivity of the AuNP probes for Cu^{2+} in the presence of Zn^{2+}, Pb^{2+}, Na^{+}, K^{+}, Hg^{2+}, Mg^{2+}, Ni^{2+}, Cd^{2+}, and Ca^{2+} (0.1 mM, respecctively). (b) Plot of $\Delta I_s/I_{s0}$ vs. Cu^{2+} concentration.

In summary, we use a functionalized AuNP probe to study the translocation of AuNP through a solid-state nanopore. The surface of AuNPs are modified with Rhod-DPA, a rhodamine derivative molecule without fluorescence. Once in the presence of Cu^{2+}, the fluorescence of Rhod-DPA can be activated due to the binding between Rhod-DPA and Cu^{2+}, which changes the configuration of Rhod-DPA molecule on AuNP surface, thus inducing the PRET from AuNP to Rhod-DPA. The scattering intensity of AuNPs quickly decreased after the addition of Cu^{2+}, confirming the translocation of nanoparticles. The obtained results demonstrate the successful establishment of our tracking strategy, providing a potential tool for the design of different analytical sensors based on single nanoparticle translocation.

This research was supported by the National Natural Science Foundation of China (21327807, 51375092), the Science Fund for Creative Research Groups (21421004), the National Science Fund for Distinguished Young Scholars of China (21125522, 21575041), and the China Postdoctoral Science Foundation (2015M570335).

Notes and references

1 J. Li; M. Gershow, D. Stein, E. Brandin, J. A. Golovchenko, *Nat. Mater.* **2003**, 2, 611–5.
2 P. Chen, J. Gu, E. Brandin, Y. R. Kim, Q. Wang, D. Branton, *Nano Lett.* **2004**, 4, 2293–2298.
3 J. B. Heng, C. Ho, T. Kim, R. Timp, A. Aksimentiev, Y. V. Grinkova, S. Sligar, K. Schulten, G. Timp, *Biophys. J.* **2004**, 87, 2905–11.
4 D. Fologea, M. Gershow, B. Ledden, D. S. McNabb, J. A. Golovchenko, J. Li, *Nano Lett.* **2005**, 5, 1905–1909.
5 G. M. Skinner, M. van den Hout, O. Broekmans, C. Dekker, N. H. Dekker, *Nano Lett.* **2009**, 9, 2953–60.
6 S. M. Iqbal, D. Akin, R. Bashir, Nat. Nanotech. 2007, 2, 243–8.
7 M. van den Hout, I. D. Vilfan, S. Hage, N. H. Dekker, *Nano Lett.* **2010**, 10, 701–7.
8 K. J. Freedman, M. Jürgens, A. S. Prabhu, C. W. Ahn, P. Jemth, J. B. Edel, M. J. Kim, *Anal. Chem.* **2011**, 83 (13), 5137–5144.

9 D. Japrung, J. Dogan, K. J. Freedman, A. Nadzeyka, S. Bauerdick, T. Albrecht, M. J. Kim, P. Jemth, J. B. Edel, *Anal. Chem.* **2013**, 85, 2449−2456.
10 A. R. Hall, S. van Dorp, S. G. Lemay, C. Dekker, *Nano Lett.* **2009**, 9, 4441−4445.
11 S. W. Kowalczyk, A. R. Hall, C. Dekker, *Nano Lett.* **2009**, 10, 324−328.
12 F.-N. Meng, X. Y. Yao, Y.-L. Ying, J. J. Zhang, H. Tian, Y.-T. Long, *Chem. Commun.*, **2015**, 51, 1202.
13 R. Mulero, A. S. Prabhu, K. J. Freedman, M. J. J. Assoc. Kim, *Lab. Automat.* **2010**, 15, 243−252,
14 H. Yamazaki, S. Ito, K. Esashika, T. Saiki, *Appl. Phys. Express* **2016**, 9, 017001.
15 K. E. Venta, M. B. Zanjani, X. C. Ye, G. Danda, C. B. Murray, J. R. Lukes, M. DrndićA, *Nano Lett.* **2014**, 14, 5358−5364.
16 L. Bacri, A. G. Oukhaled, B. Schiedt, G. Patriarche, E. Bourhis, J. Gierak, J. Pelta, L. Auvray, *J. Phys. Chem. B* **2011**, 115, 2890–2898.
17 K. Matsui, I. Yanagi, Y. Goto, K.Takeda, *Sci. Rep.* **2015**, 5, 17819.
18 M. Tsutsui, Y. H. He, K.Yokota, A. Arima, S. Hongo, M.Taniguchi, T. Washio, T. Kawai, *ACS Nano* DOI: 10.1021/acsnano.5b05906.
19 M. P. Cecchini, A.Wiener, V. A. Turek, H. Chon, S. Lee, A. P. Ivanov, D. W. McComb, J. Choo, T. Albrecht, S. A. Maier, J. B. Edel, *Nano Lett.* **2013**, 13, 4602−4609.
20 L. Lesser-Rojas, P. Ebbinghaus, G. Vasan, M.-L. Chu, A. Erbe, C.-F. Chou. *Nano Lett.* **2014**, 14, 2242−2250.
21 Y. Li, C. Chen, S. Kerman, P. Neutens, L. Lagae, G. Groeseneken, T. Stakenborg, P. V. Dorpe, *Nano Lett.* **2013**, 13, 1724−1729.
22 G. Goyal, K. J. Freedman, M. J. Kim, *Anal. Chem.* **2013**, 85, 8180−8187.
23 A. Ivankin, R. Y. Henley, J. Larkin, S. Carson, M. L. Toscano, M. Wanunu, *ACS Nano* **2014**, 10, 10774-10781.
24 T. Gilboa, A. MellerE. *Analyst*, **2015**, 140, 4733–4747.
25 K. Imura, K. Ueno, H. Misawa, H. Okamoto, *Nano Lett.* **2011**, 11, 960–965.
26 A. Barik, L. M. Otto, D. Yoo, J. Jose, T. W. Johnson, S.-H. Oh, *Nano Lett.* **2014**, 14, 2006−2012.
27 G. L. Liu, Y.-T. Long, Y. Choi, T. Kang, L. P. Lee, *Nat. Methods* **2007**, 4, 1015-1017;
28 C. Jing, L. Shi, X. Y. Liu, Y.-T. Long; *Analyst*, **2014**, 139, 64;
29 L. Shi, C. Jing, Z. Gu, Y.-T. Long, *Sci. Rep.* **2015**, 5, 10142.
30 Z.-Q. Hua, X.-M. Wang, Y.-C. Feng, L. Ding, H.-Y. Lu, *Dyes and Pigments* **2011**, 88, 257-261.
31 Y. H. Li, Y. R. Zhao, W. H. Chan, Y. J. Wang, Q. H. You, C. H. Liu, J. Zheng, *Anal. Chem.* **2015**, 87, 584−591.
32 W Wang, N.-K. Wong, M. Sun, C. Q. Yan, S. Y. Ma, Q. B. Yang, Y. X. Li, *ACS Appl. Mater. Interfaces*, **2015**, 7 (16), 8868–8875.